Supplement 1: Attachment of tracking devices

Fig. S1. Attachment of a geolocator (Intigeo-C65, Migrate Technology) on a plastic band on a long-tailed jaeger. © Yannick Seyer

Fig. S2. Attachment of a satellite transmitter (PTT-100 Microwave Telemetry) on the back of a long-tailed jaeger. © Denis Sarrazin

Supplement 2: Deployment information of tracking devices

Table S1. Summary of the deployment period of all geolocators (geo) recovered and satellite transmitters (sat) deployed on Bylot Island (n_{geo} = 40; n_{sat} = 10) and on Igloolik Island (n_{geo} = 2). Last date of recording: date the device stopped working if it was not working at recovery.

Sex	Device type	Device ID[a]	Site deployed	Date deployed	Date recovered	Last day of recording	No days of recording
U[b]	sat	84009	Bylot	Jul. 9, 2008	-	Aug. 27, 2008	49
U	sat	84014	Bylot	Jul. 9, 2008	-	Oct. 12, 2008	95
F	sat	84007	Bylot	Jul. 1, 2008	-	*NA*[c]	0
F	sat	84008	Bylot	Jul. 12, 2008	-	Sep. 4, 2008	54
F	sat	84010	Bylot	Jul. 11, 2008	-	Aug. 22, 2008	42
F	sat	84011	Bylot	Jul. 2, 2008	-	Aug. 29, 2008	59
F	sat	84012	Bylot	Jul. 5, 2008	-	Sep. 27, 2008	85
F	sat	84013	Bylot	Jul. 1, 2008	-	Sep. 9, 2008	70
F	sat	84015	Bylot	Jul. 2, 2008	-	Aug. 16, 2008	46
F	sat	84016	Bylot	Jul. 10, 2008	-	Sep. 21, 2008	74
F	geo	F634	Bylot	Jul. 6, 2014	Jun. 25, 2016	Dec. 7, 2015	519
F	geo	F637	Bylot	Jul. 7, 2014	Jun. 26, 2015	Jun. 12, 2015	340
F	geo	F638	Bylot	Jul. 7, 2014	Jun. 23, 2015	Mar. 13, 2015	341
F	geo	F641	Bylot	Jul. 8, 2014	Jun. 27, 2016	Mar. 25, 2015	260
F	geo	F915	Bylot	Jul. 5, 2014	Jun. 26, 2015	-	356
F	geo	R833	Bylot	Jun. 23, 2015	Jun. 25, 2016	-	368
F	geo	R834	Bylot	Jun. 25, 2015	Jun. 27, 2016	-	368
F	geo	R838	Bylot	Jul. 4, 2015	Jun. 27, 2016	Apr. 25, 2016	296
F	geo	R840	Bylot	Jul. 5, 2015	Jun. 22, 2019	-	0
F	geo	R842	Bylot	Jul. 7, 2015	Jul. 6, 2016	-	365
F	geo	R846	Bylot	Jul. 8, 2015	Jun. 27, 2016	-	355
F	geo	R847	Bylot	Jul. 8, 2015	Jul.5, 2016	-	363
F	geo	R849	Bylot	Jul. 8, 2015	Jul. 5, 2016	-	363
F	geo	R850	Bylot	Jul. 9, 2015	Jul. 9, 2016	-	366
F	geo	X568	Bylot	Jun. 23, 2016	Jun. 24, 2017	Mar. 5, 2017	255
F	geo	X569	Bylot	Jun. 24, 2016	Jun. 22, 2019	Aug. 19, 2016	56
F	geo	X571	Bylot	Jun. 30, 2016	Jun. 21, 2017	Dec. 18, 2016	171
F	geo	X576	Bylot	Jul. 5, 2016	Jun. 25, 2018	Dec. 23, 2016	171
F	geo	X584	Bylot	Jul. 10, 2016	Jun. 25, 2019	Mar. 5, 2017	238
F	geo	X595	Igloolik	Jul. 8, 2016	Jul. 7, 2017	Dec. 11, 2016	156
F	geo	BK188	Bylot	Jun. 25, 2018	Jun. 23, 2019	-	363
M	geo	F636	Bylot	Jul. 6, 2014	Jun. 24, 2016	Aug. 7, 2014	32
M	geo	F639	Bylot	Jul. 7, 2014	Jun. 23, 2016	Jan. 21, 2016	563
M	geo	F643	Bylot	Jul. 9, 2014	Jun. 28, 2019	Nov. 24, 2015	503
M	geo	F908	Bylot	Jun. 30, 2014	Jun. 25, 2015	-	360
M	geo	F909	Bylot	Jun. 30, 2014	Jun. 23, 2016	Jul. 26, 2015	391
M	geo	F913	Bylot	Jul. 5, 2014	Jul. 3, 2015	-	363
M	geo	R837	Bylot	Jul. 4, 2015	Jun. 21, 2019	Dec. 18, 2016	533
M	geo	R839	Bylot	Jul. 4, 2015	Jun. 27, 2016	-	359
M	geo	R843	Bylot	Jul. 7, 2015	Jun. 27, 2018	Dec. 14, 2016	526

Sex	Device type	Device ID[a]	Site deployed	Date deployed	Date recovered	Last day of recording	No days of recording
M	geo	R845	Bylot	Jul. 8, 2015	Jun. 27, 2016	-	355
M	geo	R848	Bylot	Jul. 8, 2015	Jul. 5, 2016	-	363
M	geo	X567	Bylot	Jun. 20, 2016	Jun. 19, 2017	Oct. 9, 2016	110
M	geo	X570	Bylot	Jun. 30, 2016	Jun. 21, 2017	Mar. 22, 2017	264
M	geo	X575	Bylot	Jul. 5, 2016	Jun. 26, 2019	-	0
M	geo	X578	Bylot	Jul. 6, 2016	Jun. 28, 2017	Dec. 16, 2016	163
M	geo	X582	Bylot	Jul. 8, 2016	Jul. 5, 2019	Jan. 14, 2017	189
M	geo	X583	Bylot	Jul. 10, 2016	Jul. 5, 2019	Aug. 30, 2016	52
M	geo	X585	Bylot	Jul. 10, 2016	Jul. 5, 2017	Nov. 7, 2016	119
M	geo	X596	Igloolik	Jul. 8, 2016	Jul. 10, 2017	Jan. 5, 2017	180
M	geo	BK187	Bylot	Jun. 25, 2018	Jun. 26, 2019	-	366
M	geo	BK191	Bylot	Jun. 27, 2018	Jun. 23, 2019	-	360

[a]Four birds were equipped with different geolocators on different years (F913 & R837, R850 & X584, X578 & BK191, X585 & BK187).

[b]Sex unknown

[c]The bird never left Bylot Island

Supplement 3: Details on the geolocator analysis method

Analysis of geolocator data

We estimated sunset and sunrise using the threshold method (Ekstrom 2004, Lisovski & Hahn 2012) with the *TwGeos* package (Lisovski et al. 2016) in *R*. We set the threshold value to 1.15 lux, the lowest value we could use to avoid noise with the night-time light levels. Because on-site calibration of geolocators is impossible due to 24-h daylight during summer in the Arctic, we performed a 7 to 16 d calibration in an open field in southern Quebec (46°44'N, 71°28'W) in May and/or June to determine a zenith angle. As we were expecting the birds to be in different habitats (land vs. sea) and at very different latitudes during summer and winter, we calculated a different zenith angle on the wintering site, a stationary period during which average shading intensity should be constant (Lisovski et al. 2012). For 19 migratory tracks, we used the open-field calibration zenith angle during the breeding period, the Hill-Ekstrom calibration zenith angle (Lisovski et al. 2012) during the wintering period, and the mean of these zenith angles during migratory periods. For 24 migratory tracks, we obtained very unlikely locations with this approach, thus we only used the open-field calibration zenith angle. Estimated zenith angles ranged from 93.0° to 99.3°.

To determine the geographic locations, we analyzed light-level data using a Bayesian approach with the SGAT package (Wotherspoon et al. 2013), which uses the Metropolis algorithm to create its Markov Chain Monte Carlo simulations (Sumner et al. 2009). We used three independent chains with 1000 samples for the burn-in distribution, 900 samples for the tuning distribution, and 2000 samples to define the posterior distribution. Each sample represents one set of estimated geographic locations. We provided the model with 1) raw location estimates calculated with the threshold method, 2) a spatial mask where the likeliness of the position decreased gradually inland, up to 5 times less likely >100 km inland than over the sea, but not impossible, and 3) a movement model defining probable flight speed following a gamma distribution (mean = 1.4, sd = 0.08). We assumed a mean travel speed of 14 km h^{-1} with a maximum at 61 km h^{-1} (Spear & Ainley 1997, Sittler et al. 2011). To avoid too long and unrealistic paths, we limited the time available to travel between consecutive twilights between 7 to 12 h. This was necessary for 19 tracks, especially around equinoxes when twilight estimation is less accurate because of equal day length (Lisovski & Hahn 2012), or when convergence of the model was impossible. While this approach discarded unrealistic latitudinal estimation, some uncertainty persisted around the equinoxes.

Migration phenology and characterization

Since long-tailed jaegers become entirely terrestrial during the breeding period, we expected a sudden change in the number of immersion events when they switched from the marine to the terrestrial environment, and vice versa. To estimate the departure and arrival dates on the breeding site, we used the immersion data as suggested by Fauchald et al. (2019). Because these data are recorded at relatively short intervals, we smoothed them before further analysis. We summed the wet events daily and calculated a 3-d running mean (*caTools* package; Tuszynski 2020). We used the *cpt.meanvar* function from the package *changepoint* (Killick & Eckley 2014, Killick et al. 2016) with a binary

segmentation algorithm (Scott & Knott 1974). A visual inspection of changepoint plots allowed us to select the transitions corresponding to the beginning of the fall migration and the end of the spring migration. We validated these dates with the first location estimated after the departure from the breeding site, and the last one recorded at the end of the migration respectively. Usually, these locations were south of Baffin Island because of the 24-h daylight in summer. When the first location recorded out of the breeding site was prior to the departure date estimated by the changepoint method (n = 3; mean difference of 1.7 d), we chose the one estimated from the location.

To define fall and spring stopovers, we looked at the stationary periods estimated by the *ChangeLight* function (*GeoLight* package; Lisovski & Hahn 2012). We used a minimum stationary period of 3 consecutive days and a probability threshold for site change (quantile) of 0.85. We used the *mergeSites* function to join stationary periods separated by single outliers and a maximum distance threshold of 200 km.

To define wintering period, we used a three-step approach based on the MATCHED (Migratory Analytical Time Change Easy Detection) method (Chen et al. 2016, Doko et al. 2016). First, we performed a changepoint analysis to identify sudden changes in an ordered sequence of data for three parameters: latitude, longitude, and net-squared displacement (NSD), which corresponds to the straight-line distance between the starting location (i.e. the breeding site), and any other subsequent location. The changepoint analysis with a binary segmentation algorithm marked the changes in mean and variance (*cpt.meanvar*) for these three parameters (Fig. S3). During the wintering period, we expected the three parameters to present flat and stable lines as birds should be staying in the same region. Since jaegers are coming back to the same breeding site, we were expecting a double sigmoid function between these parameters and time over a full-year period (Bunnefeld et al. 2011). Second, a visual inspection of these parameters (latitude, longitude, NSD) plotted with the migratory path helped to identify the beginning and the end of the wintering period. Finally, we validated the dates with those estimated from the stationary periods revealed by the *ChangeLight* function for the same time period (i.e. winter).

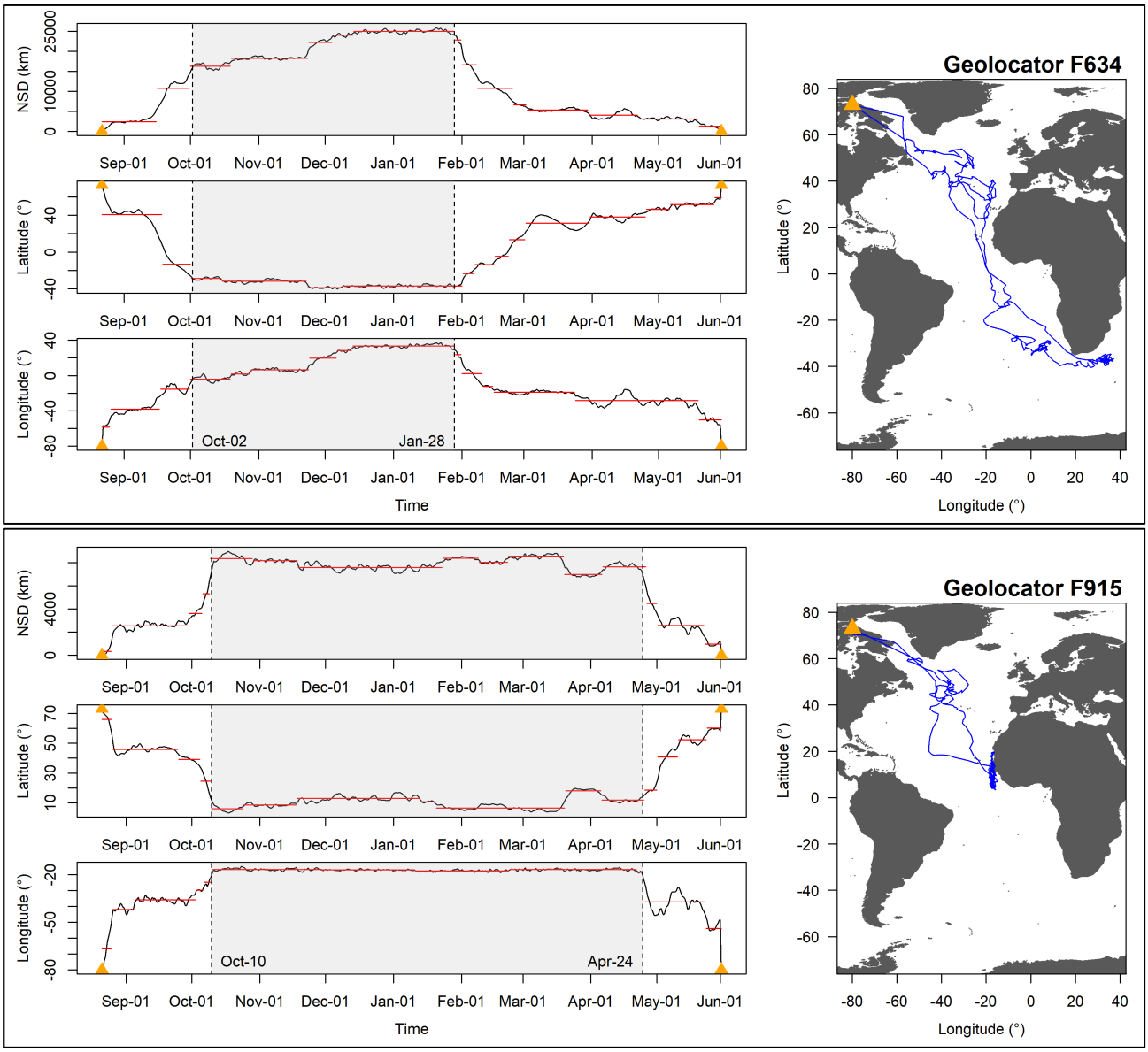

Fig. S3. Annual pattern of three movement parameters, net-squared displacement (NSD), latitude and longitude, for two individuals marked with geolocators on Bylot Island. The red lines display the segments identified by the binary segmentation changepoint analysis, which are separated by sudden changes in parameter values. The grey shaded area represents the wintering period defined by the visual inspection of the changepoints for NSD, latitude and longitude together, and validated by the migratory path (blue line). The orange triangle represents the breeding site, and the period individuals are at the site.

Table S2. Optimal value of smoothing parameter (*h*) estimated by the bivariate normal kernel method and the least-square cross-validation algorithm for the individual and population kernel distribution estimations in long-tailed jaegers during the fall and spring stopover and wintering periods.

Parameter		Individual	Population
Fall		0.39 – 1.88	0.68
Winter		0.17 – 0.90	0.35
Spring		0.46 – 1.08	0.73
Male	Fall	-	0.67
	Winter	-	0.30
	Spring	-	0.80
Female	Fall	-	0.75
	Winter	-	0.42
	Spring	-	0.71

Literature cited

Bunnefeld N, Börger L, van Moorter B, Rolandsen CM, Dettki H, Solberg EJ, Ericsson G (2011) A model-driven approach to quantify migration patterns: individual, regional and yearly differences. J Anim Ecol 80:466–476.

Chen W, Doko T, Fujita G, Hijikata N, Tokita K, Uchida K, Konishi K, Hiraoka E, Higuchi H (2016) Migration of tundra swans (*Cygnus columbianus*) wintering in Japan using satellite tracking: identification of the eastern palearctic flyway. Zoolog Sci 33:63–72.

Doko T, Chen W, Higuchi H (2016) Development of MATCHED (Migratory Analytical Time Change Easy Detection) method for satellite-tracked migratory birds. ISPRS Ann Photogramm Remote Sens Spatial Inf Sci III–2:61–68.

Ekstrom PA (2004) An advance in geolocation by light. Mem Natl Inst Polar Res, Spec Issue 58:210–226.

Fauchald P, Tarroux A, Bråthen VS, Descamps S, Ekker M, Helgason HH, Merkel B, Moe B, Åström J, Strøm H (2019) Arctic-breeding seabirds' hotspots in space and time - A methodological framework for year-round modelling of environmental niche and abundance using light-logger data. NINA Report 1657. Norwegian Institute for Nature Research, Tromsø.

Killick R, Eckley IA (2014) Changepoint: an R package for changepoint analysis. J Stat Softw 58:1–19.

Killick R, Haynes K, Eckley IA (2016) Changepoint: An R package for changepoint analysis. R package version 2.2.2.

Lisovski S, Hahn S (2012) GeoLight – processing and analysing light-based geolocator data in R. Methods Ecol Evol 3:1055–1059.

Lisovski S, Hewson CM, Klaassen RHG, Korner-Nievergelt F, Kristensen MW, Hahn S (2012) Geolocation by light: accuracy and precision affected by environmental factors. Methods Ecol Evol 3:603–612.

Lisovski S, Wotherspoon S, Sumner M (2016) TwGeos: Basic data processing for light-level geolocation archival tags. R package version 0.1.2.

Scott AJ, Knott M (1974) A cluster analysis method for grouping means in the analysis of variance. Biometrics 30:507–512.

Sittler B, Aebischer A, Gilg O (2011) Post-breeding migration of four long-tailed skuas (*Stercorarius longicaudus*) from North and East Greenland to West Africa. J Ornithol 152:375–381.

Spear LB, Ainley DG (1997) Flight speed of seabirds in relation to wind speed and direction. Ibis 139:234–251.

Sumner MD, Wotherspoon SJ, Hindell MA (2009) Bayesian estimation of animal movement from archival and satellite tags. PLoS ONE 4:e7324.

Tuszynski J (2020) CaTools: Tools: Moving Window Statistics, GIF, Base64, ROC AUC, etc. R package version 1.18.0.

Wotherspoon S, Sumner M, Lisovski S (2013) R package SGAT: solar/satellite geolocation for animal tracking. R package version 0.1.3.

Supplement 4: Wintering and stopover areas

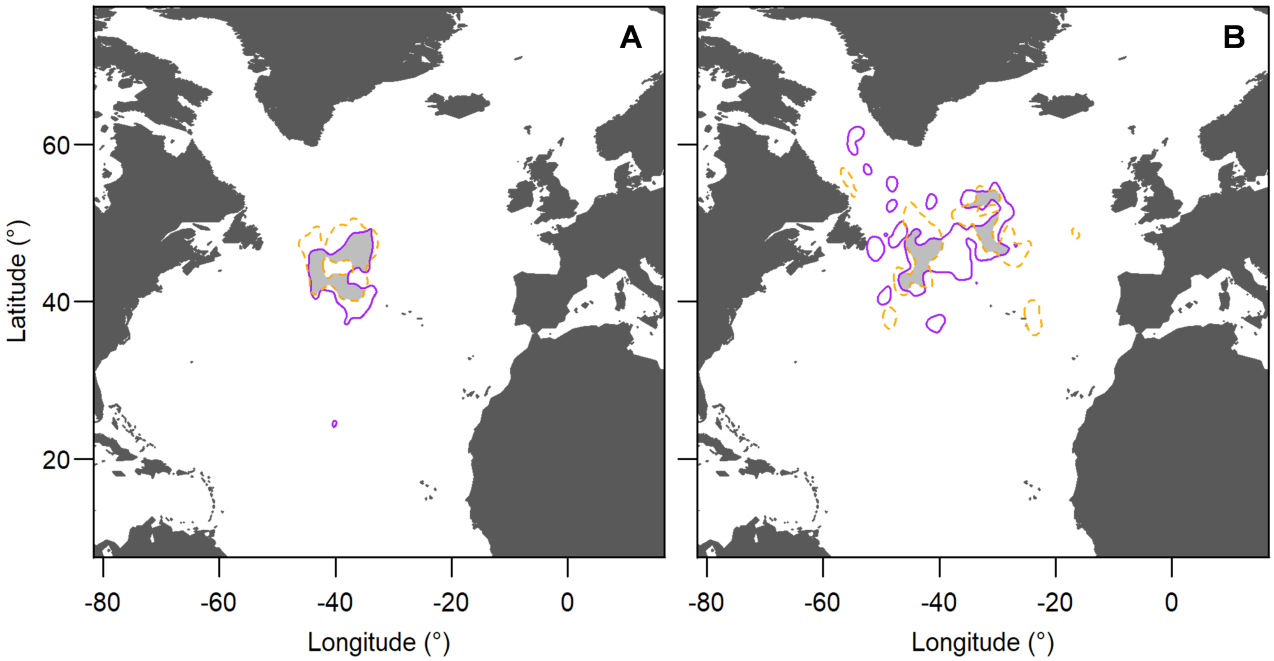

Fig. S4. A) Fall and B) spring stopover core areas of female (purple solid line) and male (orange dashed line) long-tailed jaegers recorded with geolocators. The grey shading represents the overlap between sexes. The fall stopover core area of females overlapped at 65% with the one of males and at 60% for males. During spring stopovers, these overlaps dropped respectively to 33% and 39%.

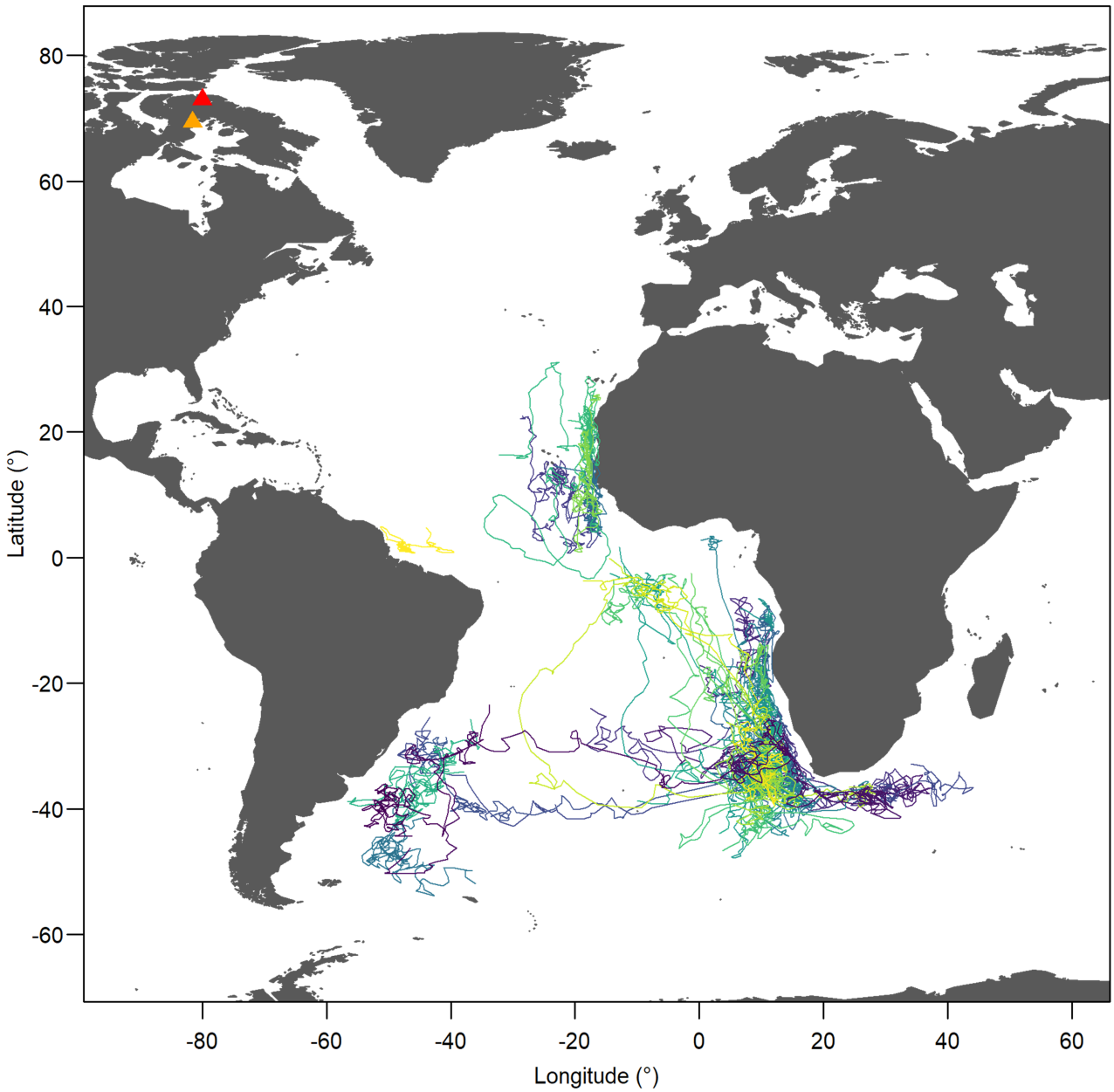

Fig. S5. Movement during the wintering period of long-tailed jaegers breeding in the eastern Canadian Arctic on Bylot Island (red triangle) and Igloolik Island (orange triangle) and recorded with geolocators. Each color represents a different individual.

Table S3. Within-pair comparison of the migration phenology and wintering sites used by long-tailed jaegers breeding in the eastern Canadian Arctic and recorded with geolocators. Pairs were nesting together at deployment and at recovery (pair 1-4) or sighted together if they were not nesting (pair 5-6). Wintering sites: main site comes first. *NA*: Information not available due to device failure.

Pair	ID	Sex	Departure from breeding site	Wintering sites	Arrival at breeding site
1	F915	F	Aug 20	Canary C.	Jun. 5
	F913	M	Aug 21	Benguela C.	Jun. 1
2	R838	F	Aug 20	Benguela C.	*NA*
	R839	M	Aug 20	Benguela C.	Jun. 10
3	R846	F	Aug 8	Brazil C.	May 30
	R845	M	Aug 16	Benguela C.	Jun. 1
4	R847	F	Aug 10	Canary C.	Jun. 13
	R848	M	Aug 14	Canary C.	Jun. 5
5	X571	F	Aug 2	Benguela C.	*NA*
	X570	M	Aug 6	Canary C.	*NA*
6	BK188	F	Jul 27	Benguela C./Brazil C.	May 27
	BK187	M	Aug 10	Brazil C.	Jun. 2

Supplement 5: Output of linear models

Table S4. Slope parameters (β) and their 95% confidence intervals (CI) of models examining the links between different movement parameters and sex, stage of the annual cycle or wintering sites of long-tailed jaegers or tracking device. R^2_m: Marginal R-squared for fixed effects (linear mixed-effect models) or adjusted R-squared (linear models). R^2_c: Conditional R-squared for fixed and random effects. *n*: Sample size.

Response variable	Explanatory variables[a]	β	Low CI	High CI	R^2_m	R^2_c	*n*
Total distance traveled[b]	Spring migration	2935	1346	4523	0.14	0.47	63
Total distance traveled[c]	Male	-248.4	-6063.6	5566.9	0.05	-	23
Size of the wintering core area[c]	Male	-67128	-156338	22082	0.05	-	26
Travel speed[d]	Fall migration	236.3	212.2	260.4	0.72	0.74	164
	Fall stopover	40.9	15.9	65.8			
	Spring migration	115.0	87.4	142.6			
	Spring stopover	50.8	20.1	81.4			
Fall migration travel speed[c]	Male	-36.9	-92.7	18.9	0.04	0.04	42
Spring migration travel speed[c]	Male	22.8	-26.2	71.7	0.00	-	26
Fall migration travel speed[e]	Agulhas C.	16.7	-144.5	177.9	0.02	0.02	39
	Benguela C.	-13.5	-136.8	109.8			
	Brazil C.	20.1	-151.8	192.0			
	Guinea C.	-16.0	-176.2	144.1			
	North Equatorial C.	-46.4	-258.3	165.4			
Spring migration travel speed[e]	Agulhas C.	-55.8	-130.8	19.3	0.39	-	26
	Benguela C.	-9.5	-65.2	46.2			
	Brazil C.	14.9	-60.1	89.9			
	Guinea C.	-149.0	-234.1	-64.0			
Fall migration travel speed	Departure date from breeding site	-1.37	-5.18	2.43	0.02	0.02	42
Spring migration travel speed	Departure date from winter site	1.08	0.43	1.73	0.30	-	26
Fall migration travel speed[f]	Satellite transmitters	42.9	-40.0	125.8	0.02	0.02	49
Daily immersions[d]	Fall migration	-950.2	-1062.9	-837.5	0.70	0.72	164
	Fall stopover	-893.7	-1010.9	-776.4			
	Spring migration	-315.1	-446.5	-183.8			
	Spring stopover	-146.7	-290.8	-2.6			

Response variable	Explanatory variables[a]	β	Low CI	High CI	R^2_m	R^2_c	*n*
Daily immersions in spring[g]	Stopover	214.1	47.1	381.1	0.08	0.45	66
	Migration after stopover	199.6	32.6	366.6			
Daily immersions[b]	Travel speed	-2.11	-2.77	-1.45	0.79	0.85	67
	Spring migration	1034.0	602.4	1465.6			
	Travel speed x Spring migration	-2.55	-4.02	-1.08			

[a]Date were expressed as day of the year for statistical analyses.
Reference levels: [b]Fall migration; [c]Female; [d]Wintering period; [e]Canary C.; [f]Geolocators; [g]Migration before stopover

Table S5. Slope parameters (β) and their 95% confidence intervals (CI) of models examining the links between chlorophyll *a* concentration and wintering or stopover sites of long-tailed jaegers. R^2: adjusted R-squared. *n*: Sample size.

Response variable	**Explanatory variables**	**β**	**Low CI**	**High CI**	**R^2**	***n***
Chlorophyll *a* concentration[a]	Agulhas C.	-0.57	-0.62	-0.52	0.92	114
	Benguela C.	-0.68	-0.73	-0.64		
	Brazil C.	-0.50	-0.54	-0.45		
	Guinea C.	-0.77	-0.82	-0.72		
	North Equatorial C.	-0.58	-0.63	-0.53		
Chlorophyll *a* concentration[b]	Spring stopover	0.58	0.53	0.64	0.93	37

Reference levels were as follow: [a]Canary C.; [b]Fall stopover

Table S6. Slope parameters (β) and their 95% confidence intervals (CI) of models examining the links between migration phenology and sex or wintering site of long-tailed jaegers or tracking device. Wintering site refers to the furthest site reached during the winter. R^2_m: Marginal R-squared for fixed effects (linear mixed-effect models) or adjusted R-squared (linear models). R^2_c: Conditional R-squared for fixed and random effects. *n*: Sample size.

Response variable[a]	**Explanatory variables**	**β**	**Low CI**	**High CI**	**R^2_m**	**R^2_c**	***n***
Departure from breeding site[b]	Male	4.19	-1.18	9.55	0.06	0.06	43
Departure from breeding site[c]	Satellite transmitters	6.28	0.13	12.43	0.08	0.08	50
Arrival to fall stopover[c]	Satellite transmitters	-1.02	-8.84	6.80	0.00	0.14	44
Duration of the fall stopover[d]	Male	7.41	0.54	14.28	0.52	0.52	40
	Agulhas C.	-21.78	-37.63	-5.92			
	Benguela C.	-18.97	-30.99	-6.96			
	Brazil C.	4.13	-12.65	20.91			
	Guinea C.	-17.11	-34.58	0.36			
	North Equatorial C.	-10.33	-32.75	12.08			
Arrival to wintering site[d]	Male	9.93	-3.07	22.92	0.11	0.54	40
	Agulhas C.	-8.10	-37.36	21.17			
	Benguela C.	-1.81	-24.16	20.54			
	Brazil C.	6.12	-23.54	35.79			
	Guinea C.	-1.55	-37.51	34.41			
	North Equatorial C.	-4.97	-44.83	34.88			
Departure from wintering site[d]	Male	16.86	-3.15	36.88	0.48	-	26
	Agulhas C.	-60.27	-97.12	-23.43			
	Benguela C.	-39.96	-67.23	-12.68			
	Brazil C.	-42.27	-79.12	-5.43			
	Guinea C.	-81.82	-124.61	-39.03			
Duration of the wintering period[d]	Male	7.8	-18.8	34.4	0.21	-	26
	Agulhas C.	-52.0	-100.9	-3.1			
	Benguela C.	-37.2	-73.4	-1.0			
	Brazil C.	-49.0	-98.0	-0.1			
	Guinea C.	-76.5	-133.3	-19.7			
Duration of the spring stopover[d]	Male	-14.94	-28.70	-1.18	0.30	-	23
	Agulhas C.	37.06	9.78	64.35			
	Benguela C.	10.01	-8.07	28.10			
	Brazil C.	10.07	-14.10	34.25			
	Guinea C.	13.82	-22.07	49.71			

Response variable[a]	Explanatory variables	β	Low CI	High CI	R^2_m	R^2_c	*n*
Arrival to breeding site[d]	Male	-0.57	-4.62	3.48	0.02	-	23
	Agulhas C.	-5.00	-13.03	3.03			
	Benguela C.	-4.93	-10.26	0.39			
	Brazil C.	-3.10	-10.21	4.02			
	Guinea C.	0.71	-9.85	11.28			
Duration of migration and stopover combined[e]	Spring migration	21.5	9.7	33.2	0.16	0.21	69

[a]Date were expressed as day of the year for statistical analyses

Reference levels were as follow: [b]Female; [c]Geolocators, [d]Female and Canary C.; [e]Fall migration

Supplement 6: Chlorophyll concentration

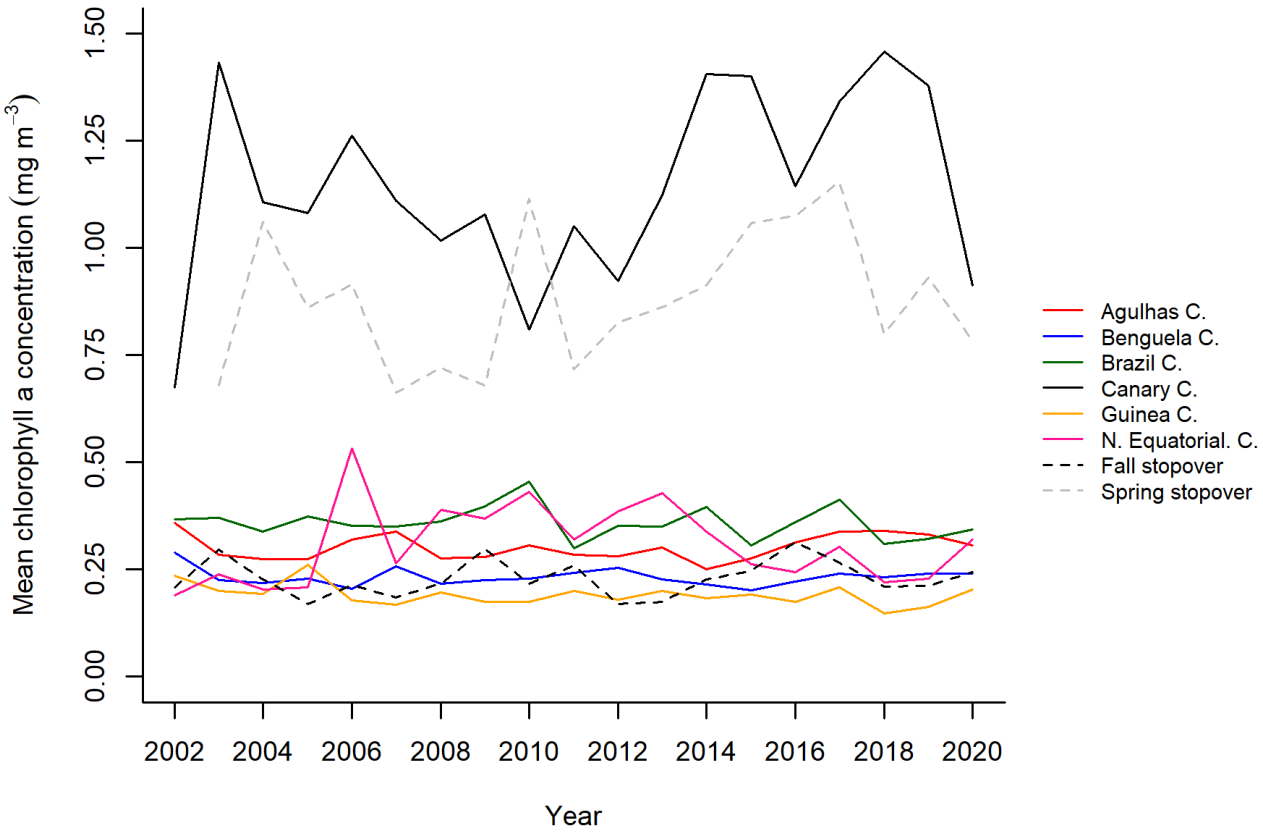

Fig. S6. Mean annual chlorophyll *a* concentration estimated for the wintering sites (solid line) used by long-tailed jaegers breeding on Bylot Island and Igloolik Island and mean chlorophyll *a* concentration estimated over 32 d for the North Atlantic stopover sites (dashed line) during fall and spring stopover periods. Chlorophyll *a* data were estimated from NASA OB DAAC (2018) (https://oceancolor.gsfc.nasa.gov/l3/).

Literature cited

NASA OB DAAC (2018) NASA Goddard Space Flight Center, Ocean Ecology Laboratory, Ocean Biology Processing Group. Moderate-resolution Imaging Spectroradiometer (MODIS) Aqua Chlorophyll Data; 2018 Reprocessing. https://oceancolor.gsfc.nasa.gov/l3/ (accessed 29 March 2021).

Supplement 7: Phenology of the annual cycle

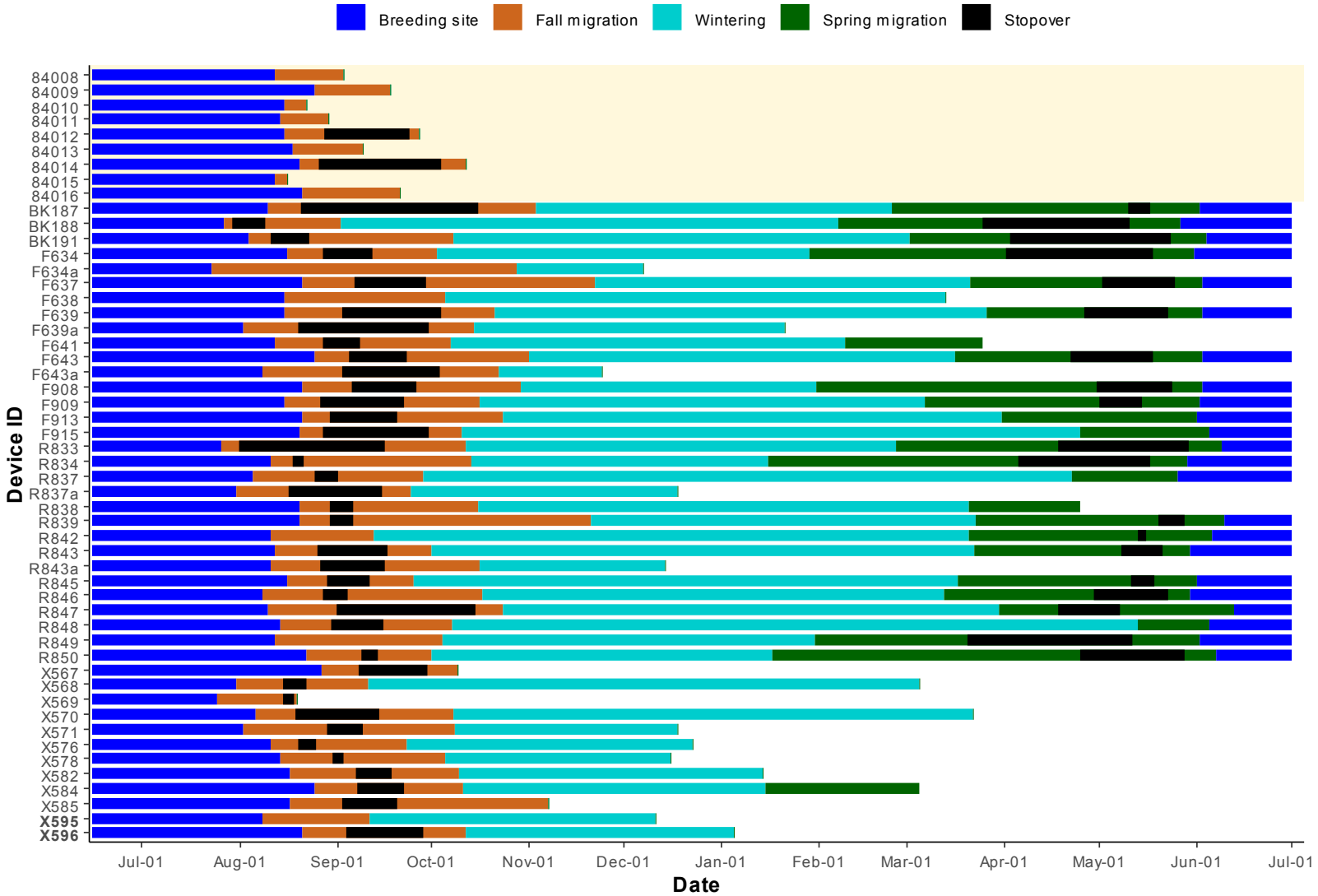

Fig. S7. Phenology of the annual cycle of long-tailed jaegers recorded with satellite transmitters (yellow shaded area) or geolocators breeding on Bylot Island or Igloolik Island (device IDs X595 and X596 at bottom, in bold).